The large-scale structures in turbulent plane Couette flow

By M. J. Lee

Turbulent plane Couette flow has been numerically simulated at a Reynolds number, $\mathrm{Re} = U_w h/\nu = 6{,}000$. Preliminary examination of the instantaneous velocity and vorticity fields revealed the existence of large-scale eddies which grow in the flow direction with time and have the spanwise scale as large as the channel-height. The persistence of the longitudinal eddies was not observed when the small scales in the spanwise direction were not well resolved, indicating that the growth of the large-scale longitudinal eddies requires the contribution from the small-scale motions in the spanwise direction. The statistical correlations in the flow agree well with the experimental results.

1. Introduction: motivation and objectives

An important fluid-mechanical aspect of a fully-developed plane Couette flow is that the flow has a constant shear stress across the entire channel height, be it laminar or turbulent. The constancy of shear stress, $\tau/\rho = \nu\, dU/dy - \overline{uv}$ (equal to its value at the wall, $\tau_w/\rho = \nu\, dU/dy|_w$), is a direct consequence of zero mean pressure gradient in the flow as it is driven by shear generated at two plane, solid boundaries in rectilinear, parallel movement (at speed U_w) relative to each other (see Figure 1). Here, (x, y, z) denote the coordinates in the flow direction, in the normal direction to the center plane of the channel (i.e. $-1 \leq y/h \leq 1$, where h is the channel half-height) and in the spanwise direction, respectively. In a fully-developed plane Couette flow, turbulence statistics are uniform in a horizontal xz-plane. Because of its simple flow geometry and the existence of the constant shear-stress region, turbulent plane Couette flow has been considered as one of the building-block flows for study of wall-bounded turbulent shear flows.

Another characteristic of plane Couette flow is that both the mean vorticity (or mean shear, $S = dU/dy$) and turbulent shear stress ($-\rho\,\overline{uv}$) are symmetric about the center plane ($y/h = 0$), in contrast with pressure-driven Poiseuille flow that has profiles antisymmetric about $y/h = 0$. Because of the resulting finite production rate, $-S\,\overline{uv}$, even in the core region (say, $0.2\text{–}0.5 \leq y_\perp/h \leq 1$, where $y_\perp$ is the distance normal to a nearest wall) the shapes of the turbulence intensity profiles ($\overline{u^2}$, $\overline{v^2}$, $\overline{w^2}$) differ significantly among the three components (see El Telbany & Reynolds 1982), indicating the existence of a high degree of anisotropy in the flow. Therefore, we conjecture (or hypothesize) that instantaneous turbulence structures in the core region of plane Couette flow would be quite different from those of Poiseuille flow. This question has not been addressed before. However, in the vicinity of the walls (e.g. $y_\perp/h \leq 0.1\text{–}0.2$), turbulence structures

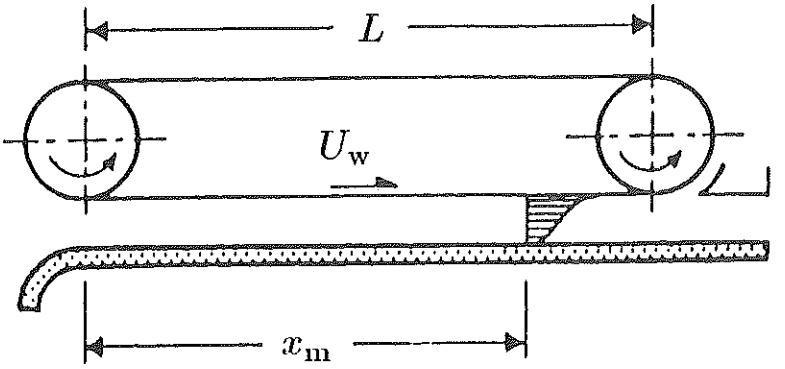

FIGURE 1. Schematic diagram of a typical experimental setup of turbulent plane Couette flow. Because the belt is prone to deform at high speeds, the length of the shearing boundary has to be limited, resulting in a rather short flow-development length (or time), $x_m/h = 10$–300.

of the two flows are expected to be similar, since the near-wall dynamics of a turbulent shear flow is primarily controlled by a mechanism universally represented by the 'law of the wall.' For instance, the near-wall turbulence structures in boundary layer and plane Poiseuille flow appear to be identical even though the outer structures of the two flows are significantly different.

Despite its apparent importance as a paradigm of wall-bounded turbulent shear flows, plane Couette flow has not been studied extensively. In most previous experiments (Reichardt 1956, 1959; Robertson 1959; Robertson & Johnson 1970; Leutheusser & Chu 1971; El Telbany & Reynolds 1980, 1981), the boundary shearing was realized by employing either a (flexible) moving belt or a fluid interface, which is prone to deform at high speeds (or at high Reynolds numbers, $\mathrm{Re} = U_w h/\nu$). To alleviate this problem, the length of the shearing boundary had to be made short, which resulted in a rather short flow-development length (or time): $x_m/h = 10$–300 (x_m is the distance from the entrance to the location of the principal measuring station). Because of the difficulties arising from the movement of the shearing boundary, only the profiles of mean velocity, turbulence intensities and turbulent shear stress were obtained in most experiments, and measurements of energy spectra and two-point velocity correlations were limited in the streamwise direction only (Robertson & Johnson 1970; Aydin & Leutheusser 1979, 1989).

The present study aims at two main objectives. First, we would like to identify turbulence structures in plane Couette flow and examine differences from those in plane Poiseuille flow. Previous works showed that the core region of

plane Poiseuille flow is dominated by hairpin-shaped vortical eddies (Moin & Kim 1985; Kim & Moin 1985). It is our goal to understand the mechanism by which the boundary shearing produces turbulence structures different from those generated in a pressure-driven flow. Second, we would like to test the capability of existing turbulence models (and scaling laws) in describing the turbulence characteristics of plane Couette flow. Because most near-wall turbulence models have been developed by assuming that the wall layer is of constant-stress equilibrium (Townsend 1976, §5), there is an intrinsic interest to examine the performance of existing models.

To achieve these objectives, turbulent plane Couette flow has been numerically simulated by integrating the Navier-Stokes equations in time (for a brief description, see §2.1). Using the database obtained from the direct numerical simulation, the existence of large-scale eddies in plane Couette flow was found. In this report, special attention is focused on the large-scale motions that develop in the flow direction with time and that have the cross-stream dimensions as large as the channel-height, $2h$. A discussion of the statistical correlations follows the examination of the instantaneous structures.

2. Accomplishments

2.1. Direct numerical simulation

For the present study, the flow Reynolds number ($U_w h/\nu$) of 6,000 was selected. Note that the chosen value of the Reynolds number is higher than the range of the reported critical transition Reynolds numbers, 1,000–2,000. The numerical algorithm of the present code is identical to that used in the computation of Kim, Moin & Moser (1987), except the wall boundary conditions. A spectral method (Fourier in the horizontal xz-plane and Chebyshev in the vertical y-direction) for the spatial differentiations and an Adams-Bashforth/Crank-Nicolson algorithm for time advancement were used.

Direct numerical simulation (DNS hereinafter) of a turbulent flow is meaningful only when all the essential scales in the flow under consideration are properly represented in the computation. As shown in Table 1, computations have been carried out with three different sizes (i.e. horizontal dimensions, B_x and B_z) of the computational domain (or box): $B_x/h = 4\pi$, 8π and 16π. In all the cases reported here, the number of the Chebyshev modes used for the vertical direction was 65, and the spanwise dimension was half the streamwise dimension: $B_z/B_x = \frac{1}{2}$. The largest computational domain (for runs Q1, Q2, Q3) has a high streamwise-to-vertical aspect ratio, $B_x/(2h) \simeq 25$.

A computation on a box of a given size was started on a coarse mesh with horizontal modes (NX,NZ) of 32×32, which was successively expanded up to 128×128 modes. The expansion of the horizontal modes was done after the flow reached a 'quasi-steady' state as determined by inspection of such statistics as the

Case	B_x/h	B_z/h	NX	NZ	$\Delta x/h$	$\Delta z/h$
B1	4π	2π	32	32	0.393	0.196
D1	8π	4π	32	32	0.785	0.393
D2			64	64	0.393	0.196
D3			128	128	0.196	0.0982
Q1	16π	8π	32	32	1.57	0.785
Q2			64	64	0.785	0.393
Q3			128	128	0.393	0.196

TABLE 1. Specifications of the computational box and the horizontal Fourier modes for plane Couette flow simulations. For all the runs, the number of the vertical Chebyshev modes was 65 and $\mathrm{Re} = U_w h/\nu = 6000$.

mean velocity, turbulent kinetic energy, shear stresses, two-point velocity correlations and energy spectra. Table 1 also shows the corresponding horizontal grid spacings, $(\Delta x, \Delta z)$. When the flow reached a 'quasi-steady' state the Reynolds number, $\mathrm{Re}_\tau = U_\tau h/\nu$, based on the wall-shear velocity, $U_\tau = (\nu\, dU/dy|_w)^{1/2}$, and channel half-height, h, was about 180. (Laminar Couette flow at this flow Reynolds number has $\mathrm{Re}_\tau \simeq 55$.) The size of the biggest computational domain was $B_x^+ \simeq 9{,}000$, $B_z^+ \simeq 4{,}500$, where the superscript + denotes a quantity made dimensionless by the viscous length scale, $\ell_\nu = \nu/U_\tau$.

2.2. The large-scale structures

The streamwise two-point correlations of fluctuating velocity components, (u, v, w), at the center of the channel $(y/h = 0)$ from the computation on the smallest box size, $(B_x, B_z)/h = (4\pi, 2\pi)$ are shown in Figure 2. The significant correlation of the streamwise velocity component, u, at the streamwise separations near $r_x/h = 2\pi$ indicates that the size of the computational domain is not sufficient for the largest eddies. Therefore, it was decided that the computation must be performed on a bigger computational domain.

Figure 3 shows the streamwise two-point correlations at the center plane $(y/h = 0)$ from the computation with a bigger box, $(B_x, B_z)/h = (8\pi, 4\pi)$. When the number of the horizontal modes was small with the grid spacing $(\Delta x, \Delta z)/h = (0.785, 0.393)$, the bigger box size appeared to be sufficient enough to contain large-scale motions in the flow, as indicated by the negligible correlations at large streamwise separations in Fig. 3(*a*). However, as the number of the horizontal modes increased so that the grid spacing became $(\Delta x, \Delta z)/h = (0.393, 0.196)$, the correlation of the streamwise velocity, u, was high again (see Fig. 3*b*). Comparison of the computations on the same box size but with different numbers of the horizontal modes (especially the spanwise modes) suggests

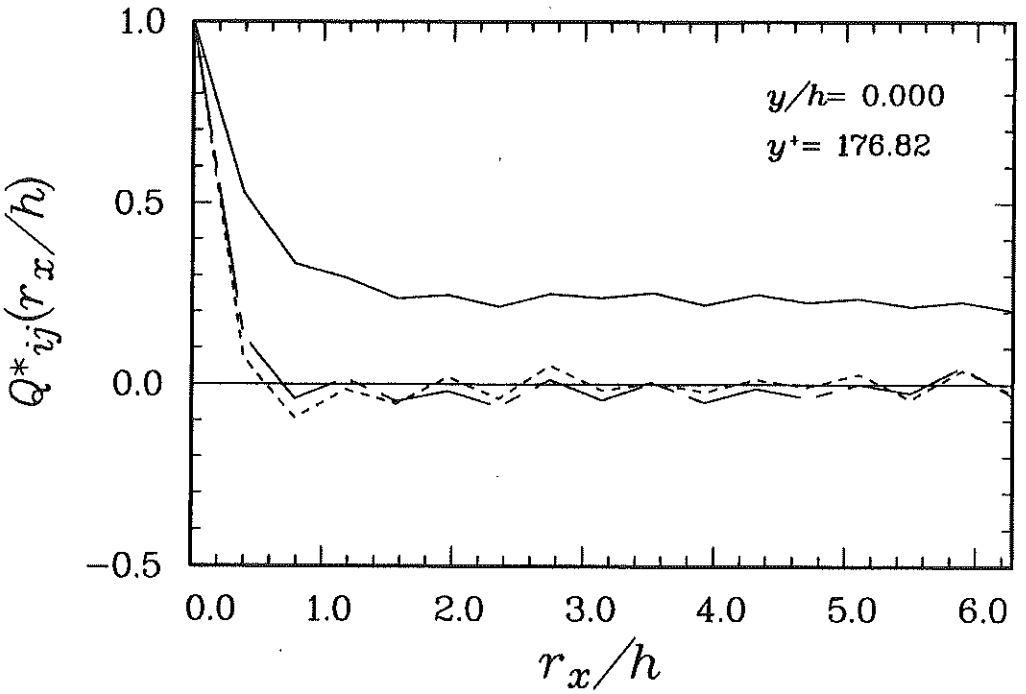

FIGURE 2. The streamwise two-point correlations of velocity at $y/h = 0$ from the computation with the smallest box, $(B_x, B_z)/h = (4\pi, 2\pi)$. ——, $Q^*_{uu}(r_x/h)$; ----, $Q^*_{vv}(r_x/h)$; ——–, $Q^*_{ww}(r_x/h)$. The significant correlation at the streamwise separation, $r_x/h = 2\pi$, indicates that the box size is insufficient to contain largest eddies in the flow. The grid spacing is $(\Delta x, \Delta z)/h = (0.393, 0.196)$.

that the growth of the longitudinal eddies requires the contribution from small-scale motions in the spanwise direction.

Inspection of the spanwise energy spectra, $E_{uu}(k_z)$, of the streamwise velocity (Figure 4, run case D3) revealed that with the contributions from small scales a definite peak develops in times at $k_z h \simeq 1$, which is an order-of-magnitude higher than the density at other scales. The presence of the sharp peak indicates the existence of a finite spanwise scale of the energetic eddies. The generating mechanism of these large-scale eddies differs significantly from that of the streaky structures in the near-wall region (sublayer) and in homogeneous shear flows (Lee, Kim & Moin 1987). The streaky turbulence structures are selectively amplified by the high mean shear rate ($S^* = Sq^2/\epsilon \gg 1$), a linear mechanism in which transfer of energy between different scales is absent (Lee & Hunt 1989).

Some details of the instantaneous structures in the computed flow are discussed below. Figure 5 shows the contours of the streamwise velocity fluctuations, u, plotted on the center plane ($y/h = 0$). The contours on the center

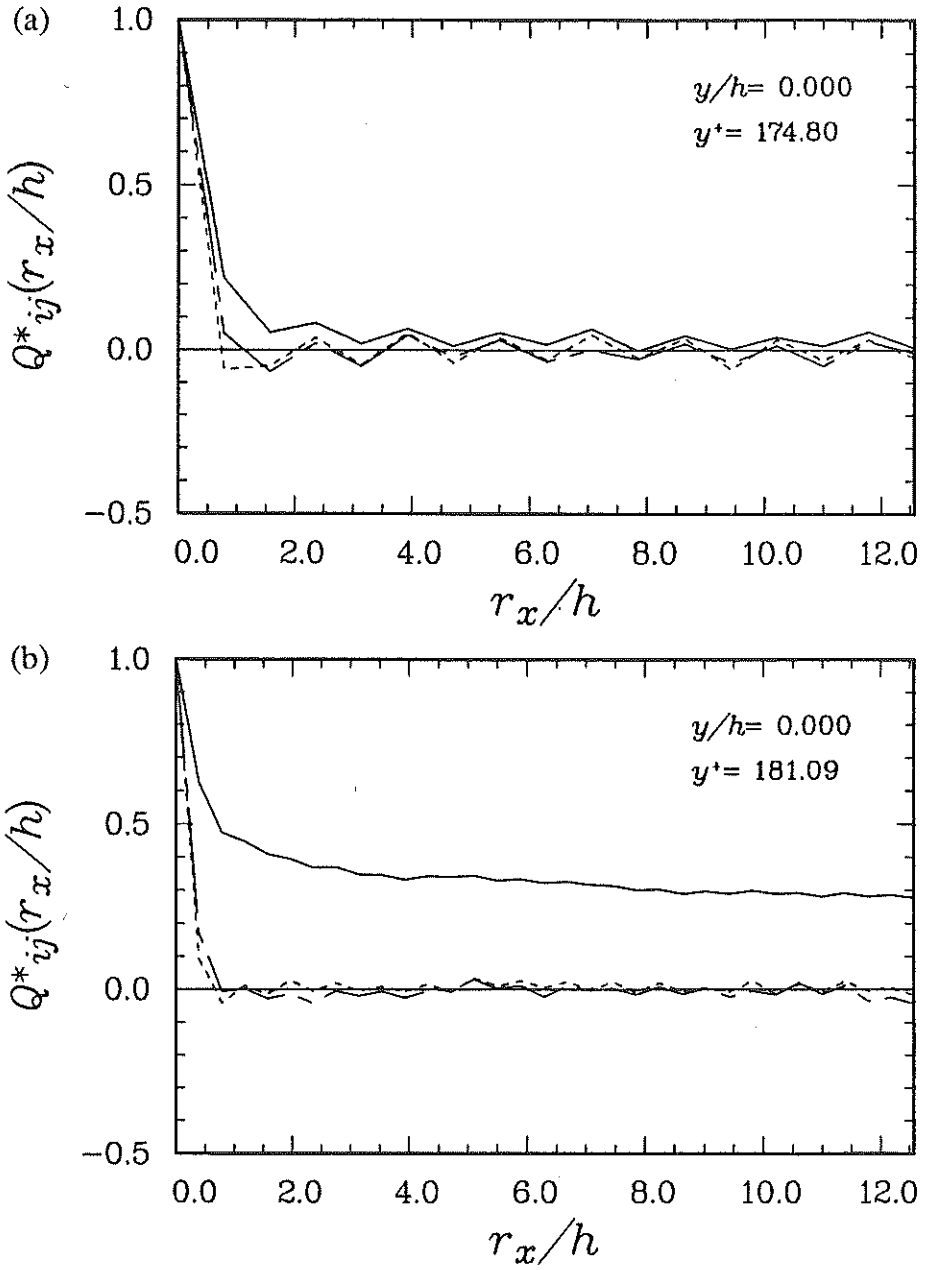

FIGURE 3. Comparison of the streamwise two-point correlations at $y/h = 0$ from the computations with different number of horizontal modes (NX,NZ) on the bigger box, $(B_x, B_z)/h = (8\pi, 4\pi)$: (*a*) (NX,NZ) = (32,32); (*b*) (NX,NZ) = (64,64). ——, $Q^*_{uu}(r_x/h)$; ----, $Q^*_{vv}(r_x/h)$; ——, $Q^*_{ww}(r_x/h)$. The development of high correlation with the increase of the number of the spanwise modes suggests that the growth of the large eddies in plane Couette flow requires contributions from the small-scale spanwise motions.

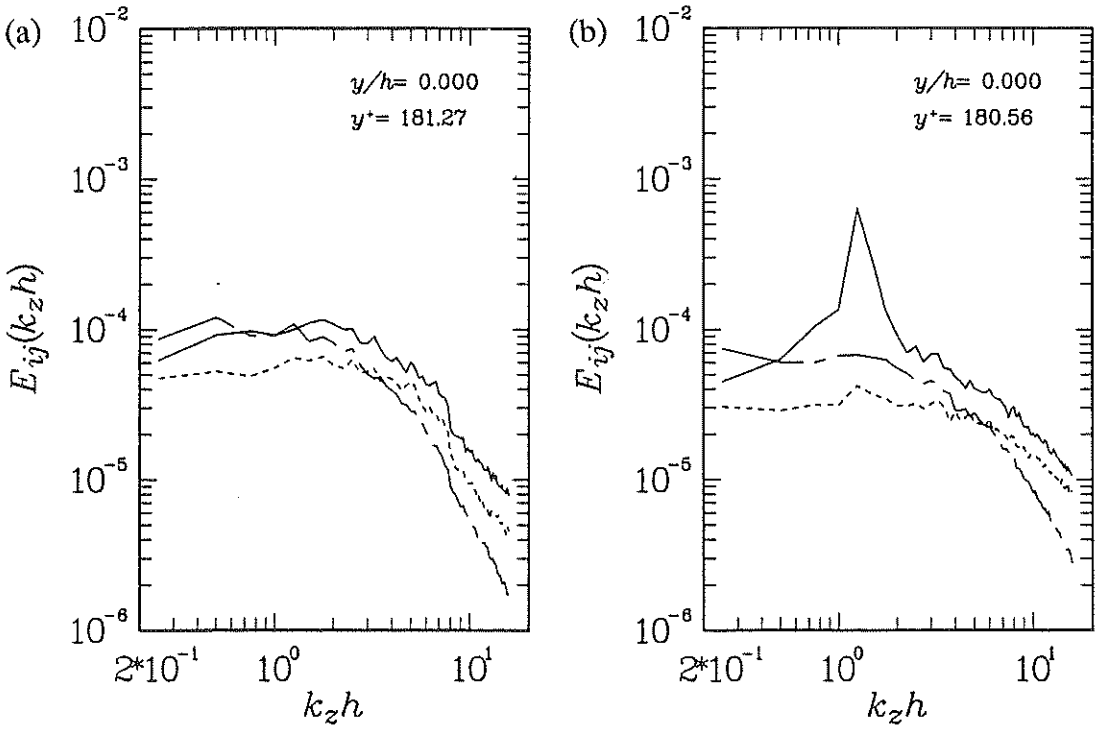

FIGURE 4. Evolution of the spanwise energy spectra at the center of the channel ($y/h = 0$), showing that the development of a peak of the streamwise component at the wavenumber $k_zh \simeq 1$: (a) earlier time, t_0; (b) later time, $(t - t_0)U_w/h \simeq$ 500–1000. ——, $E_{uu}(k_zh)$; ----, $E_{vv}(k_zh)$; ——-, $E_{ww}(k_zh)$.

plane clearly show the existence of organized large-scale eddies in the flow. The topological configuration of these structures may appear to be similar to that of the near-wall streaky structures in that the low- and high-speed flow regions are highly elongated in the flow direction and alternate in the spanwise direction. However, the length scales, Λ_x and Λ_z, of the structures in the core region are much larger than those, λ_x and λ_z, of the streaks in the sublayer: $\Lambda_x^+ \simeq 5,000$–$7,000$, $\Lambda_z^+ \simeq 900$, $\lambda_x^+ \simeq 1,000$, $\lambda_z^+ \simeq 100$, where the subscripts x and z denote the streamwise and spanwise directions, respectively. This difference in scales also suggests that the generating mechanism for the large-scale structures in the Couette flow is different from that responsible for generating the wall-layer streaks. Contours of the other velocity components (v and w), vorticity and pressure are not as much elongated, and they are more intermittent and localized in space (not shown here).

The spatial distribution of u near the two walls are different (see Figure 6). Near the bottom wall where the mean fluid speed is larger than the wall speed, the distribution of u is positively skewed, and the converse is true near the top

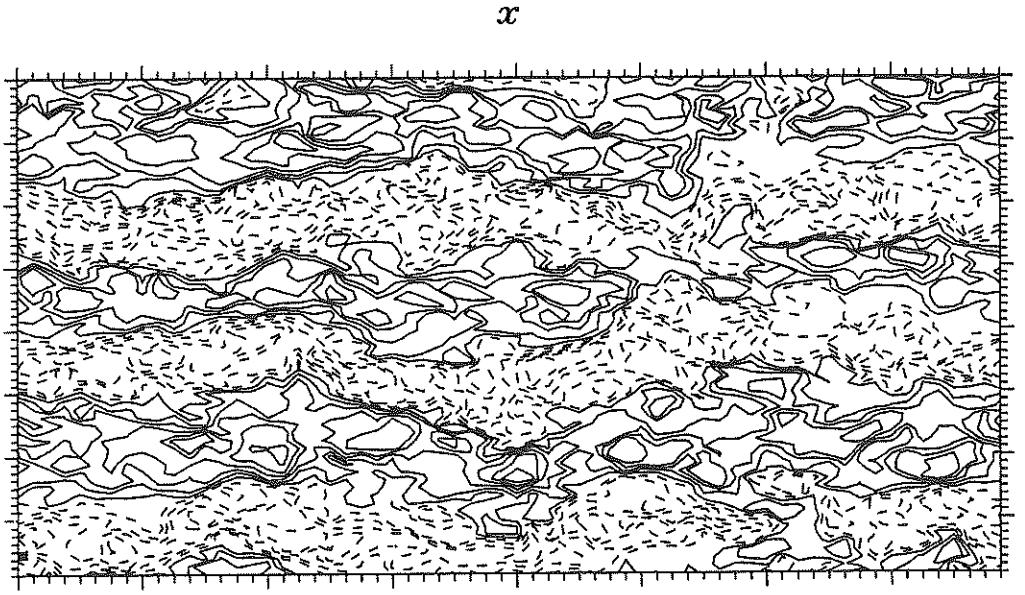

FIGURE 5. Contours of the streamwise velocity fluctuations, u, at the center of the channel ($y/h = 0$), showing the existence of large-scale structures developing in the core region. ——, $u > 0$; ----, $u < 0$.

wall. In contrast, the respective distributions of other components of velocity (v, w) and the streamwise and vertical vorticity components (ω_x, ω_y) are not as much different near the two opposite walls as the u distribution, and have skewness factors much less than that of u. However, the spanwise vorticity (ω_z) has a high negative skewness factor near the both walls.

The vertical extent of the eddy structures is shown by the contour plot of u on a yz-plane (an end view) in Figure 7. (The vertical direction is magnified by a factor of $2\frac{1}{2}$ for visual clarity near the walls; $L_z = 4\pi h$ and $Ly = 2h$.) The vertical extent of the large eddies is as big as the channel height, $2h$. The spanwise spacing between the low- or high-speed regions as determined from an inspection of contour plots such as Figure 7 is about $4h$. This is consistent with the spanwise two-point correlation of the streamwise velocity fluctuations, $Q^*_{uu}(r_z)$, that has distinct negative dips at separations $r_z/h \simeq 2$, 6 and positive peaks at $r_z/h \simeq 4$. If the computational domain were larger, the dips and peaks would appear at the separations $r_z/h = 4n - 2$ and $4n$, respectively ($n = 1$, 2, ...). However, the near-wall regions consist of small-scales structures.

2.3. Statistical correlations

Here, the statistical properties of plane Couette flow computed from the simulation with the best resolution are presented. In Figure 8(a), the computed

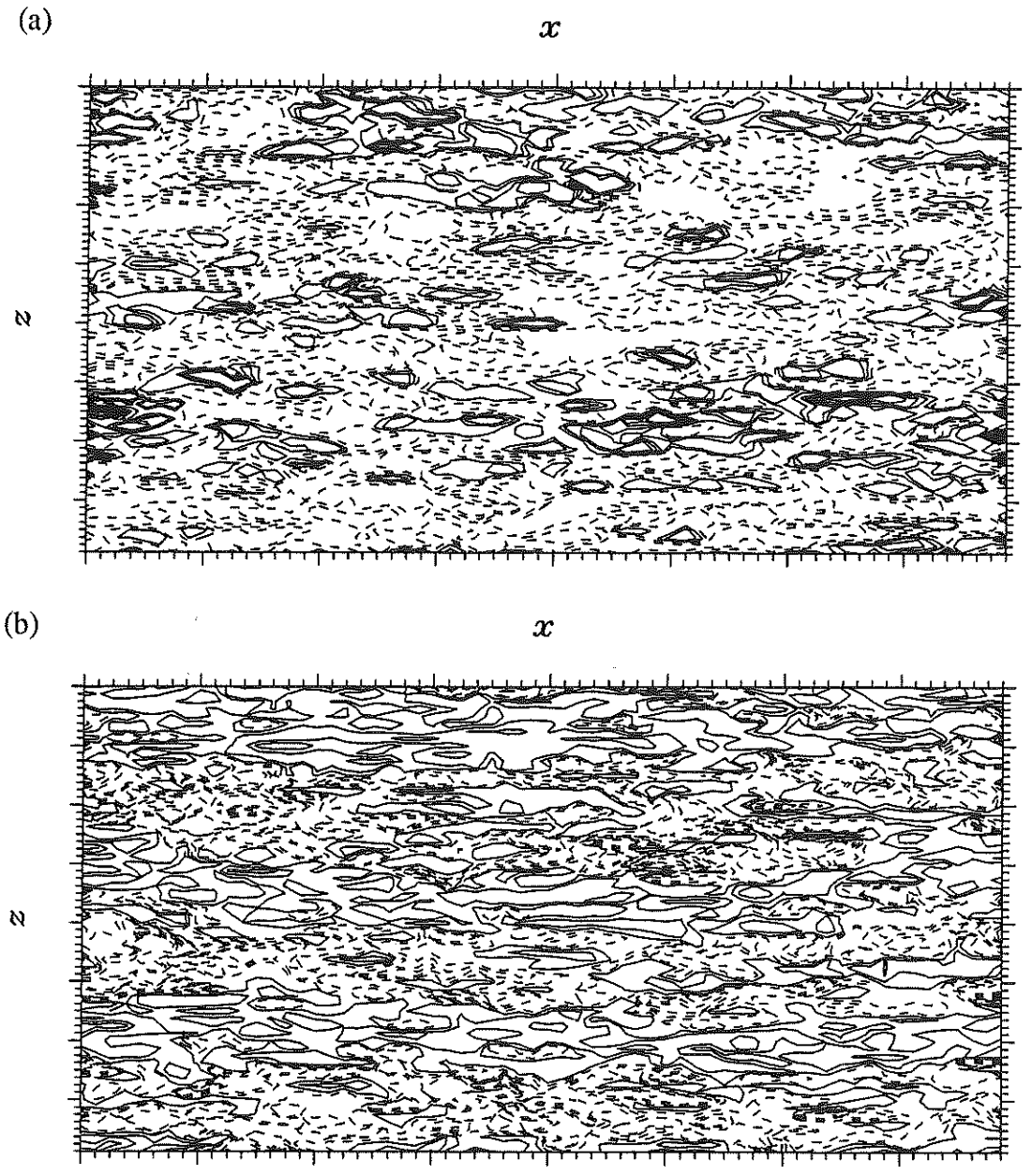

FIGURE 6. Comparison of distribution of the streamwise velocity fluctuations (*a*) near the bottom wall, $y/h = -0.98$ ($y^+ = 3.5$); (*b*) near the top wall, $y/h = +0.98$ ($y^+ = 3.5$). ——, $u > 0$; ----, $u < 0$. Note that the u-distribution is positively skewed near the bottom wall and the converse is true near the top wall.

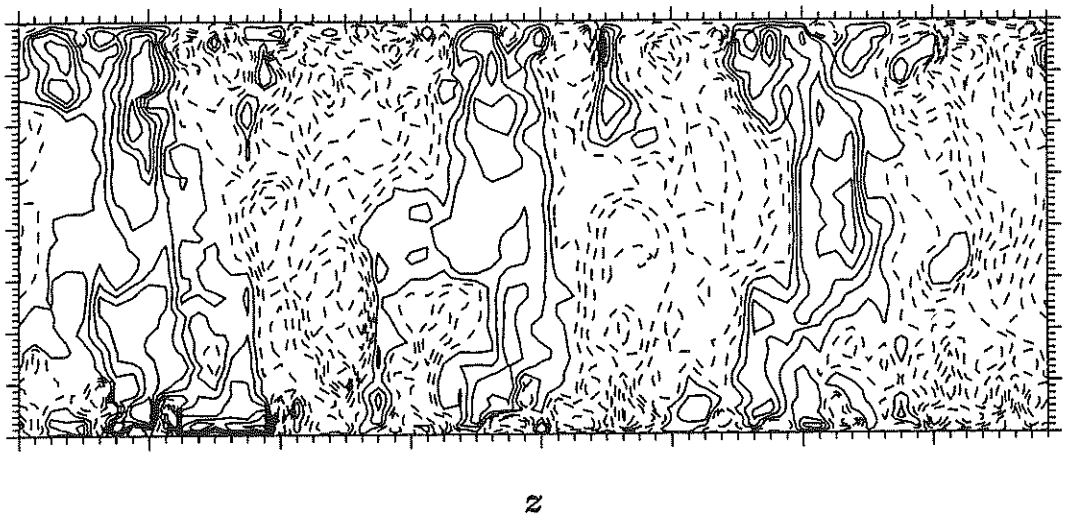

FIGURE 7. Contours of the streamwise velocity fluctuations on a yz-plane (an end view), showing that the vertical extent of the large eddies is almost the channel height ($2h$) and the spanwise spacing (or the size) of a pair is about $4h$. ——, $u > 0$; ----, $u < 0$. (Note that the vertical direction is magnified by a factor of $2\frac{1}{2}$ for visual clarity near the walls.)

mean velocity profile across the channel is compared with the experiments conducted at different flow Reynolds numbers (Re = 2,900, Reichardt 1959; Re $\simeq 2 \times 10^4$–4×10^4, El Telbany & Reynolds 1980). It should be noticed that at high Reynolds numbers the velocity profile changes rapidly within a narrow region near the wall ($y_\perp/h \leq 0.1$), and that it has a constant slope over the half channel-height around the center ($-0.5 \leq y/h \leq 0.5$). The mean velocity gradient at the boundary, $S_w = dU/dy|_w$, grows substantially with the Reynolds number, whereas that at the center plane, $S_c = dU/dy|_{y=0}$, decreases with increasing Reynolds numbers. The mean velocity gradient (or mean shear rate) in the core region is about 5% of the wall value (or total stress) and it is about 30% of the value for a laminar flow with a linear velocity profile. Thus, the total shear stress in the turbulent case is about 10 times higher than the laminar equivalent.

The near-wall profile, U^+, made dimensionless by the wall-shear velocity (U_τ), *vs.* y^+, the distance normal to the wall scaled by the viscous length ($\ell_v = \nu/U_\tau$) is shown in Figure 8(b). The solid and chain-dashed lines are the profiles near the lower and upper walls, respectively. The dashed and dotted lines denote the universal law of the wall: $U^+ = y^+$ and $U^+ = (1/\kappa)\ln y^+ + B$ ($\kappa = 0.4$ and $B = 5.5$), respectively, which fits the experimental data at a high Reynolds number (El Telbany & Reynolds 1980). The data from the present simulation

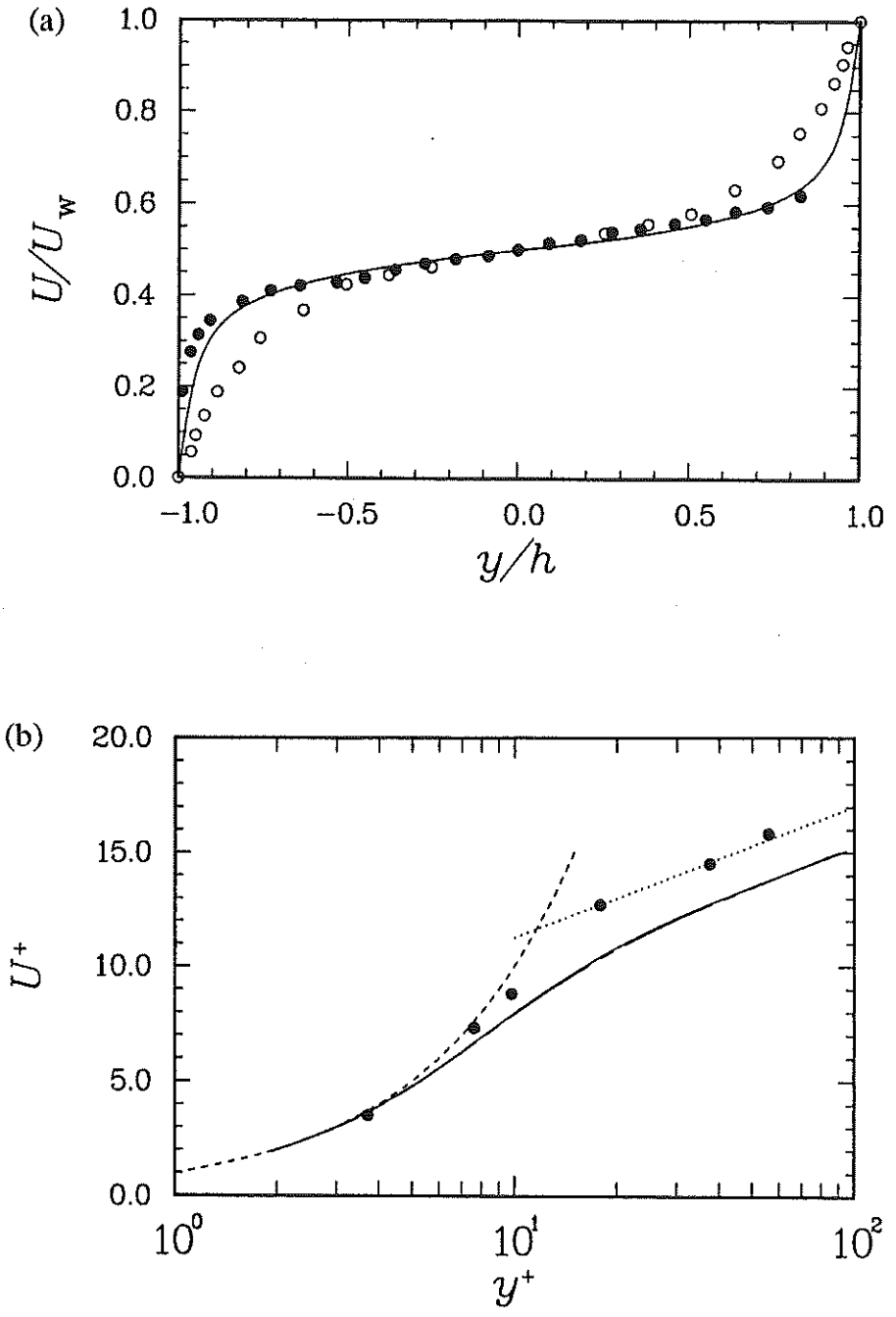

FIGURE 8. Mean velocity profile in plane Couette flow: (*a*) global profile, U/U_w *vs.* y/h; (*b*) near-wall profile, U^+ *vs.* y^+. ——, present result; ○, Reichardt (1959); ●, El Telbany & Reynolds (1980); ----, $U^+ = y^+$; ·····, $U^+ = (1/\kappa)\ln y^+ + B$ ($\kappa = 0.4$ and $B = 5.5$); In (*b*), the solid and chain-dashed lines are the profiles for the lower and upper walls, respectively.

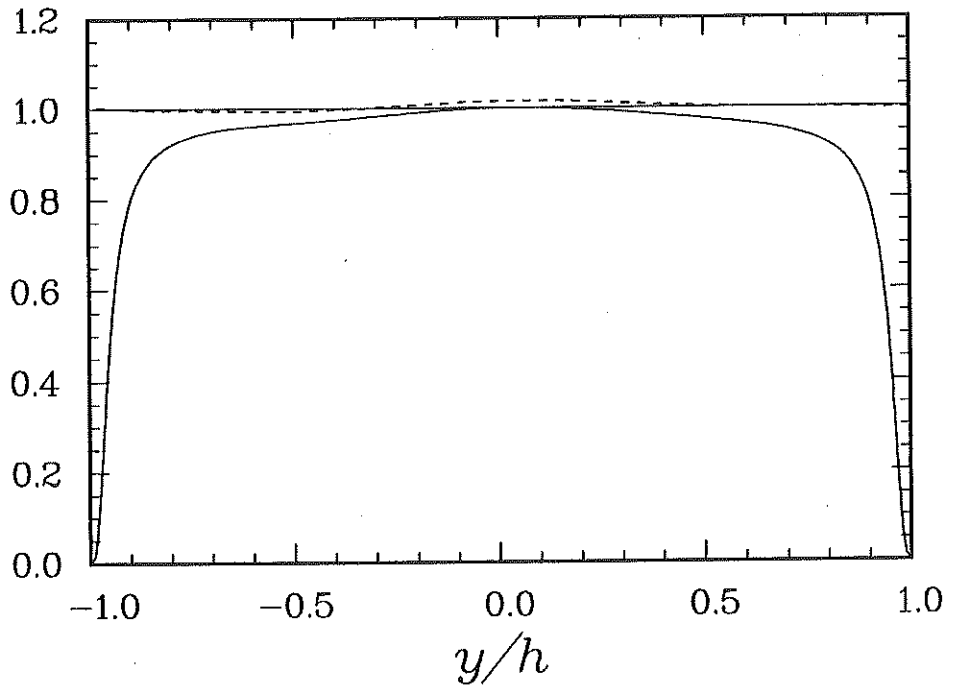

FIGURE 9. Profile of shear stresses in plane Couette flow: ——, turbulent shear stress $(-\rho\overline{uv}/\tau_w)$; ----, total shear stress (τ/τ_w).

show $B = 3.5$, a lower value than that for high Reynolds numbers ($B = 5.5$). This is counter to the usual dependence on the Reynolds number.

Figure 9 shows the profiles of turbulent and total shear stresses. The total shear stress is nearly uniform across the whole channel height. In the near-wall region, the turbulent shear stress increases rapidly with the distance from the wall: it attains $0.9\tau_w$ at $y_\perp/h = 0.2$. (The small deviation of τ/τ_w from unity is due to the insufficient number of the sample fields used for average.)

The turbulence intensities (u'^+, v'^+, w'^+) scaled by the wall-shear velocity (U_τ) in Figure 10(*a*) show good agreement with the experimental results at higher Reynolds numbers (El Telbany & Reynolds 1981). Compared with those in a plane Poiseuille flow at comparable Reynolds numbers (Fig. 10*b*, Kim *et al.* 1987), the intensities in Couette flow are significantly higher at most locations in the channel, except in the vicinity of the wall ($y^+ \leq 30$) where the Couette-flow values are higher only slightly. This marked contrast is a direct consequence of the constancy of total shear stress, $\tau = \mu\, dU/dy - \rho\overline{uv}$, across the channel in the flow. (In a plane Poiseuille flow, the total shear stress has a linear profile $\tau/|\tau_w| = -y/h$, and $dU/dy = 0$ and $\overline{uv} = 0$ at the channel center, $y/h = 0$, by symmetry.)

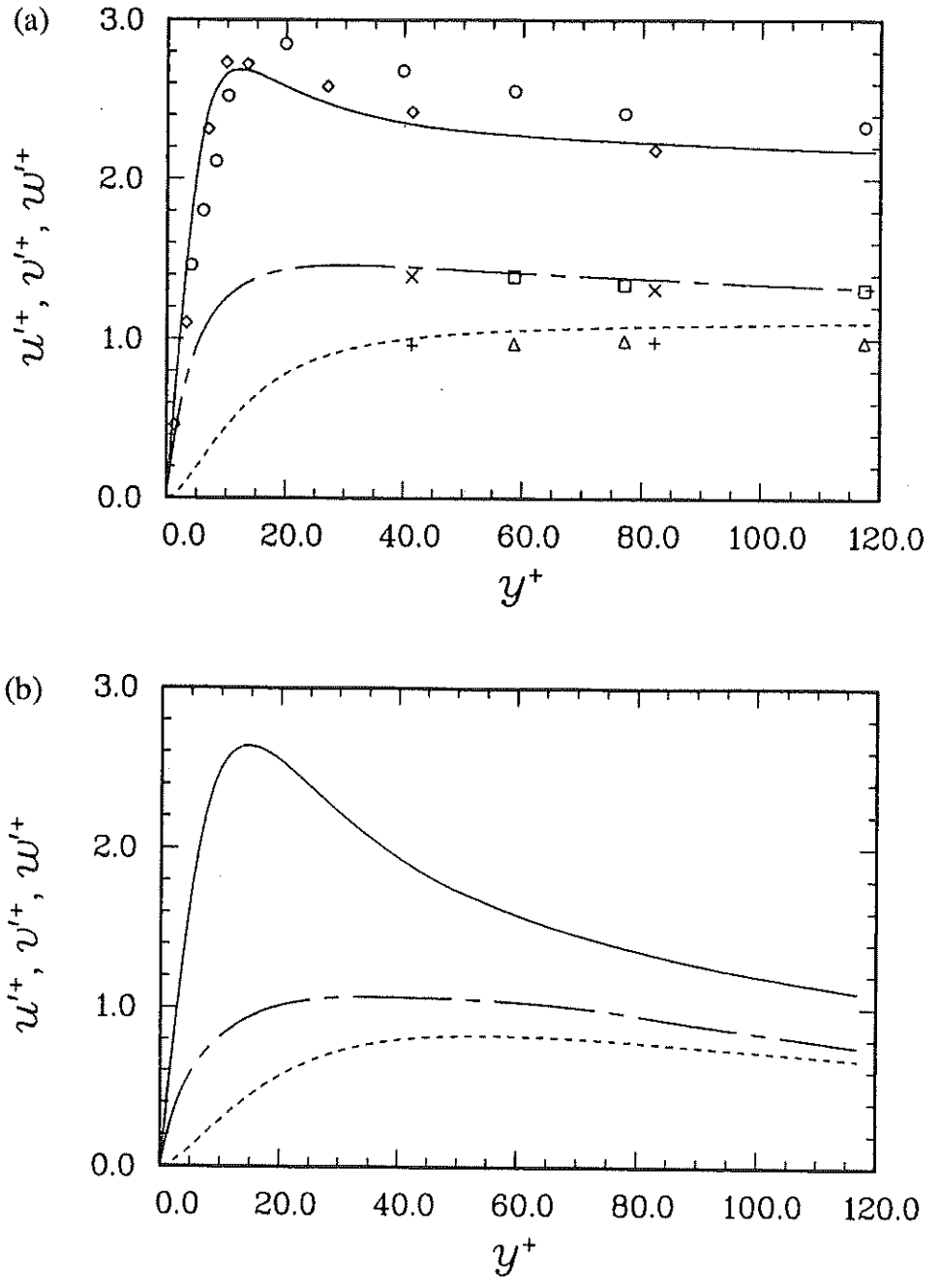

FIGURE 10. Near-wall profiles of the turbulence intensities: (u'^+, v'^+, w'^+) *vs.* y^+: (*a*) plane Couette flow; (*b*) plane Poiseuille flow. Lines are from the computations: ——, u'^+; ----, v'^+; — — —, w'^+. Symbols are the measured data from El Telbany & Reynolds (1981).

Figure 10(a) also shows that the turbulence structure in the core region has strong anisotropy, i.e. $\overline{u^2} : \overline{v^2} : \overline{w^2} \simeq 6 : 1 : 2$. The mean velocity profile is approximately linear in the core region, indicating that turbulence statistics are uniform there as would be in homogeneous turbulent flows.

3. Summary

In this report, preliminary results are presented on the existence of the large-scale structures in turbulent plane Couette flow. The structures are primarily associated with the streamwise velocity fluctuations in the core region (say, $y_\perp/h > 0.2$). These eddies develop in the flow direction in time and grow to fill the whole channel in the cross-stream plane. Analysis of the two-point correlations and spectra shows that the spanwise scale of the individual eddies is about the channel height ($2h$). The generating mechanism of these large-scale eddies differs from that of the streaky structures found in flows at high shear rate.

There is an intrinsic interest in studying plane Couette flow from the modeling point of view because this flow has a constant total shear stress across the channel. We plan to analyze turbulence statistics including the Reynolds-stress transport budget to examine the capability of the existing turbulence models. Comparison of these with those in plane Poiseuille flow would reveal the differences and similarities of the two flows in how the wall layer is affected by the structures in the core region.

REFERENCES

AYDIN, M. & LEUTHEUSSER, H. J. 1979 Novel experimental facility for the study of plane Couette flow. *Rev. Sci. Instr.* **50**, 1362–1366.

AYDIN, E. M. & LEUTHEUSSER, H. J. 1987 Experimental investigation of turbulent plane-Couette flow. *Forum on Turbulent Flows–1987*, FED vol. 51, 1987 ASME Applied Mech., Bioeng. & Fluids Eng. Conf., Cincinnati, Ohio, June 14–17, 1987 (ed. W. W. Bower), pp. 51–54. Amer. Soc. Mech. Eng.: New York.

AYDIN, E. M. & LEUTHEUSSER, H. J. 1989 Plane-Couette flow between smooth and rough walls. *J. Fluid Mech.* (*sub judice*)

EL TELBANY, M. M. M. & REYNOLDS, A. J. 1980 Velocity distributions in plane turbulent channel flows. *J. Fluid Mech.* **100**, 1–29.

EL TELBANY, M. M. M. & REYNOLDS, A. J. 1981 Turbulence in plane channel flows. *J. Fluid Mech.* **111**, 283–318.

EL TELBANY, M. M. M. & REYNOLDS, A. J. 1982 The structure of turbulent plane Couette flow. *Trans. ASME J. Fluids Eng.* **104**, 367–372.

KIM, J., MOIN, P. & MOSER, R. D. 1987 Turbulent statistics in fully developed channel flow at low Reynolds number. *J. Fluid Mech.* **177**, 133–166.

KIM, J. & MOIN, P. 1986 The structure of the vorticity field in turbulent channel flow. Part 2. Study of ensemble-averaged fields. *J. Fluid Mech.* **162**, 339–363.

KLINE, S. J., REYNOLDS, W. C., SCHRAUB, F. A. & RUNSTADLER, P. W. 1967 The structure of turbulent boundary layers. *J. Fluid Mech.* **30**, 741–773.

KREPLIN, H. & ECKELMANN, H. 1979 Behavior of the three fluctuating velocity components in the wall region of a turbulent channel flow. *Phys. Fluids* **22**, 1233.

LEE, M. J. & HUNT, J. C. R. 1989 The structure of sheared turbulence near a plane boundary. *Seventh Symp. on Turbulent Shear Flows*, Stanford University, Stanford Calif., Aug. 21–23, 1989 (ed. F. Durst *et al.*), pp. 8.1.1–8.1.6.

LEE, M. J., KIM, J. & MOIN, P. 1987 Turbulence structure at high shear rate. *Sixth Symp. on Turbulent Shear Flows*, Toulouse, France, Sept. 7–9, 1987 (ed. F. Durst *et al.*), pp. 26.6.1–26.6.6; To appear in *J. Fluid Mech.*

LEUTHEUSSER, H. J. & CHU, V. H. 1971 Experiments on plane Couette flow. *Proc. ASCE J. Hydr. Div.* **97** (HY9), 1269–1284.

MOIN, P. & KIM, J. 1985 The structure of the vorticity field in turbulent channel flow. Part 1. Analysis of instantaneous fields and statistical correlations. *J. Fluid Mech.* **162**, 339–363.

REICHARDT, H. 1956 Über die Geschwindigkeitsverteilung in einer geradlinigen turbulenten Couetteströmung. *Zeit. angew. Math. Mech.* **36**, Sonderheft 26–29.

REICHARDT, H. 1959 Gesetzmäßigkeiten der geradlinigen turbulenten Couetteströmung. *Mitteil.* No. 22. Max-Planck-Inst. Strömungsforschung und Aerodynamischen Versuchsanstalt: Göttingen.

ROBERTSON, J. M. 1959 On turbulent plane-Couette flow. *Proc. Sixth Midwestern Conf. Fluid Mech.*, Univ. of Texas, Austin, Texas, Sept. 9–11, 1959, pp. 169–182.

ROBERTSON, J. M. & JOHNSON, H. F. 1970 Turbulence structure in plane Couette flow. *Proc. ASCE J. Eng. Mech. Div.* **96** (EM6), 1171–1182.

TOWNSEND, A. A. 1976 *The structure of turbulent shear flow.* 2nd edn. Cambridge University Press: Cambridge, England.